

Switching between Proper and Hybrid-Improper Polar Structures via Cation Substitution in $A_2\text{La}(\text{TaTi})\text{O}_7$ ($A = \text{Li}, \text{Na}$).

Subhadip Mallick[†], Andrew Dominic Fortes[‡], Weiguo Zhang[§], P. Shiv Halasyamani[§], and Michael A. Hayward^{†*}

[†] Department of Chemistry, University of Oxford, Inorganic Chemistry Laboratory, South Parks Road, Oxford, OX1 3QR, UK.

[‡] ISIS Facility, Rutherford Appleton Laboratory, Chilton, Oxon OX11 0QX, UK.

[§] Department of Chemistry, University of Houston, 112 Fleming Building, Houston, Texas 77204-5003, USA.

ABSTRACT: Neutron powder diffraction data indicate that $\text{Li}_2\text{La}(\text{TaTi})\text{O}_7$ adopts a polar, $a^-a^-c^+/a^-a^-c^+$ distorted, $n = 2$ Ruddlesden-Popper structure described in space group $A2_1am$ (#36), consistent with a hybrid-improper stabilization of the polar structure via a trilinear coupling between the X_3^- , X_2^+ and Γ_5^- distortion modes. In contrast, $\text{Na}_2\text{La}(\text{TaTi})\text{O}_7$ adopts a polar, $a^-a^-c^-/a^-a^-(-c^-)$ distorted, $n = 2$ Ruddlesden-Popper structure described in space group $Pna2_1$ (#33) with the polar Γ_3^- distortion mode apparently stabilized by a second-order Jahn-Teller distortion of the $d^0 \text{Ta}^{5+}/\text{Ti}^{4+}$ cations. The change in class of polar distortion of the $A_2\text{La}(\text{TaTi})\text{O}_7$ framework, from hybrid improper (trilinearly coupled) to proper (second-order Jahn-Teller stabilized), on A-cation substitution suggests the two stabilization mechanisms are in competition in these two materials and many other hybrid improper ferroelectric phases.

Introduction

Ferroelectric materials are used in a wide range of devices from electro-optic modulators to data storage modules.¹ However, the discovery and preparation of new ferroelectric materials is challenging because in order for a phase to have a spontaneous, switchable electrical polarization it must adopt a non-centrosymmetric (NCS), polar crystal structure,^{2, 3} and centrosymmetric packing schemes tend to be energetically preferred to acentric alternatives.

A common strategy for stabilizing NCS structures is to utilize an electronically driven distortion, typically a second-order Jahn-Teller (SOJT) distortion, to lift the inversion symmetry of a material. For example, octahedrally coordinated, d^0 transition-metal cations in complex oxides (e.g. Ti^{4+} in BaTiO_3) tend to be unstable with respect to distortions which break the local inversion symmetry of the BO_6 units, driven by a mixing of the previously orthogonal metal nd and oxygen $2p$ orbitals.⁴⁻⁷ Similarly, post-transition metals (e.g. Pb^{2+} in PbTiO_3) are also susceptible to SOJT distortions (often interpreted as stereo-active lone pairs) which break the local inversion symmetry of structures, again driven by mixing of previously orthogonal empty-metal and filled-anion orbitals.⁸⁻¹³ Utilizing SOJT distortions in the pursuit of new ferroelectric materials is clearly an attractive strategy, it does however limit the chemical composition of ferroelectric materials and hampers attempts to combine ferroelectric behavior with magnetism.¹⁴

Recently there has been interest in an alternative “trilinear-coupled hybrid-improper” mechanism for stabilizing NCS phases.¹⁵ This mechanism makes use of the facile tilting and twisting distortions of the BO_6 octahedra in ABO_3 perovskite phases. By engineering suitable tilting distortions into a material, it is possible to combine two non-polar tilting modes so that they couple to, and stabilize, a third, polar distortion mode (trilinear coupling) yielding an NCS structure.¹⁵⁻¹⁷ As this mechanism does not, in principle, place any chemical constraints on a

system, it offers the prospect of broadening the chemistry of ferroelectric materials.

A symmetry analysis reveals that due to the reciprocal nature of the collective rotations of the BO_6 units in 3D ABO_3 perovskite phases, A- or B-cation order is required, in combination with suitable tilting distortions, to break the global inversion symmetry of the perovskite framework¹⁸ – a requirement that poses significant synthetic challenges.^{19, 20} However, the trilinear-coupled hybrid-improper mechanism can stabilize polar distortions in layered variants of the perovskite framework, such as $A_3B_2O_7$ $n = 2$ Ruddlesden-Popper phases²¹⁻²⁴ or $A'AB_2O_7$ $n = 2$ Dion-Jacobson phases,²⁵⁻²⁸ in the absence of cation order, so these frameworks have been the primary focus of attention.²⁹

As noted above, the trilinear-coupled hybrid-improper mechanism does not appear to impose any strong chemical constraints on ferroelectric materials. However, in practice it is generally only possible to stabilize the required large-magnitude tilting distortions, by including large B-site cations in the layered perovskite frameworks. As the ionic radius of metal cations declines across the transition series, the largest ions suitable for inclusion on the B-sites of layered perovskite oxides are early transition-metal cations in their group oxidation states. As a consequence many of the hybrid-improper ferroelectric phases reported to date contain Ti^{4+} ,²¹ Zr^{4+} ,²³ Nb^{5+} or Ta^{5+} ^{26, 30} on their B-sites. The presence of these d^0 transition-metal ions raises the prospect of competition between trilinear-coupled hybrid-improper stabilization and SOJT stabilization of polar distorted phases. Here we describe two polar $n = 2$ Ruddlesden-Popper phases, $\text{Li}_2\text{La}(\text{TaTi})\text{O}_7$ and $\text{Na}_2\text{La}(\text{TaTi})\text{O}_7$, the former stabilized by the trilinear-coupled hybrid-improper mechanism, the later by an SOJT distortion, and discuss the role of the Li^+ and Na^+ cations in mediating the competition between these two classes of polar distortion.

Experimental

Synthesis. Polycrystalline samples of $\text{Li}_2\text{La}(\text{TaTi})\text{O}_7$ and $\text{Na}_2\text{La}(\text{TaTi})\text{O}_7$ were synthesized by high-temperature solid-state synthesis from La_2O_3 (99.999%, dried at 900 °C), TiO_2 (99.995%), Ta_2O_5 (99.993%, dried at 900 °C) and Li_2CO_3 (99.999%) or Na_2CO_3 (>99%). Suitable stoichiometric ratios of the oxides were ground together in an agate mortar and pestle and mixed with either a 10% excess of Li_2CO_3 or a 5% excess of Na_2CO_3 , to compensate for the weight loss due to volatilization at high temperature. These mixtures were then placed in alumina crucibles and heated at 850 °C for 12 h in air, reground and pressed into 13 mm diameter pellets. Samples of $\text{Li}_2\text{La}(\text{TaTi})\text{O}_7$ were heated in flowing oxygen for three periods of 6 h at 1200 °C. An oxygen atmosphere is required to avoid the formation of LaTiO_3 as a secondary phase. Samples of $\text{Na}_2\text{La}(\text{TaTi})\text{O}_7$ were heated in air for three periods of 30 min at 1100 °C. This specific heating regimen was required to avoid the formation of $\text{Na}_2\text{La}_2\text{Ti}_3\text{O}_{10}$ as a secondary phase.

Characterization. Powder X-ray diffraction data were collected using a PANalytical X'pert diffractometer incorporating an X'celerator position-sensitive detector (monochromatic $\text{Cu K}\alpha_1$ radiation). High-resolution synchrotron X-ray powder diffraction (SXR) data were collected using the I11 instrument at the Diamond Light Source Ltd. Diffraction patterns were collected using Si-calibrated X-rays with an approximate wavelength of 0.826 Å from samples sealed in 0.5 mm diameter borosilicate glass capillaries. Time-of-flight neutron powder diffraction (NPD) data were collected using the HRPD diffractometer at the ISIS neutron source from the samples loaded in 8 mm diameter vanadium cans. Rietveld refinements were performed using TOPAS Academic.³¹ The powder second harmonic generation (SHG) response of samples was recorded and compared to a standard sample of $\alpha\text{-SiO}_2$. No index matching fluid was used in any of the experiments. A detailed description of the experimental setup and process has been reported previously.³²

Results

Structural Characterization of $\text{Li}_2\text{La}(\text{TaTi})\text{O}_7$. SXR and NPD data collected from $\text{Li}_2\text{La}(\text{TaTi})\text{O}_7$ can be indexed using an orthorhombic unit cell ($a = 5.496$ Å, $b = 5.511$ Å, $c = 18.229$ Å). This unit cell is consistent with an $a' = \sqrt{2}a$, $b' = \sqrt{2}b$, $c' = c$ expansion of an undistorted aristotype, $I4/mmm$ symmetry unit cell of an $n = 2$ Ruddlesden-Popper phase. Extinction conditions observed in the powder diffraction data are consistent with an A-centered unit cell. Symmetry analysis of the $n = 2$ Ruddlesden-Popper framework,^{30, 33, 34} in combination with the observation that $\text{Li}_2\text{La}(\text{TaTi})\text{O}_7$ is SHG active (activity 0.78 times $\alpha\text{-SiO}_2$) suggests an $a^-a^-c^+/a^-a^-c^+$ distorted structure^{35, 36} described in space group $A2_1am$ (#36), analogous to the reported room-temperature structure of $\text{Li}_2\text{SrNb}_2\text{O}_7$,³⁷ in which the Li^+ cations reside in tetrahedral sites within the rock salt layers. There is no evidence for any Ta/Ti ordering, so a model based on the room temperature structure $\text{Li}_2\text{SrNb}_2\text{O}_7$, but with Sr replaced by La and Nb replaced by a 1:1 disordered mixture of Ta:Ti was constructed and refined against the NPD data to achieve a good fit ($wR_p = 5.98\%$, $R_p = 5.78\%$). We also considered an $a^-a^-c^+/a^-a^-(-c^+)$ distorted structure described in space group $Pna2_1$ (#33) as structures of this type have been observed for other $\text{Li}_2\text{AB}_2\text{O}_7$ Ruddlesden-Popper phases.³⁸ The fitting statistics from the refinement of the $Pna2_1$ model ($wR_p = 5.88\%$, $R_p = 5.87\%$) are comparable to those from the $A2_1am$ structural

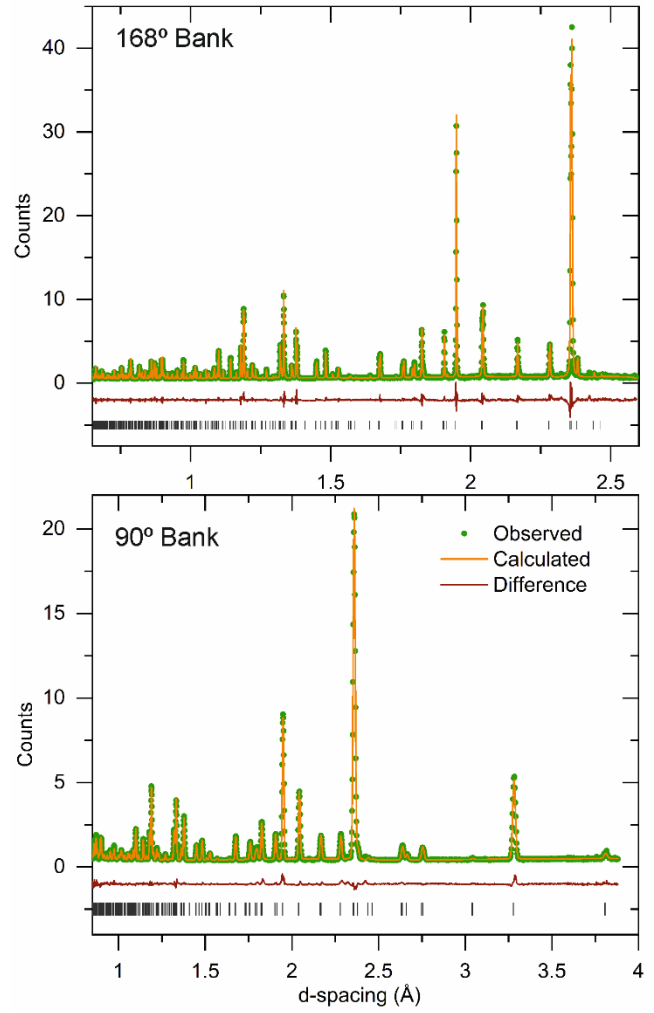


Figure 1. Observed, calculated and difference plots from the structural refinement of $\text{Li}_2\text{La}(\text{TaTi})\text{O}_7$ against NPD data collected at 298 K.

Atom	x	y	z	Occ.	Uiso (Å ²)
Li	0.6847(21)	0.0038(47)	0.2412(4)	1	0.007(2)
La	0.4345(19)	0.2406(5)	0	1	0.005(1)
Ta/Ti	0.9343(78)	0.2478(22)	0.1179(3)	0.5/0.5	0.008(2)
O(1)	0.9185(16)	0.2027(7)	0	1	0.010(1)
O(2)	0.6807(51)	0.9979(19)	0.4090(1)	1	0.007(4)
O(3)	0.1836(31)	0.0102(14)	0.8883(2)	1	0.007(4)
O(4)	0.9297(27)	0.2820(5)	0.2158(1)	1	0.009(1)
$\text{Li}_2\text{La}(\text{TaTi})\text{O}_7$ - space group $A2_1am$ (#36) $a = 5.49668(4)$ Å, $b = 5.51162(4)$ Å, $c = 18.22989(16)$ Å Formula weight = 493.60 g mol ⁻¹ , Z = 4 Radiation source: Neutron Time of Flight Temperature: 298 K $wR_p = 5.985\%$, $R_p = 5.778\%$					

Table 1. Parameters from the structural refinement of $\text{Li}_2\text{La}(\text{TaTi})\text{O}_7$ against NPD data collected at 298 K.

model ($wR_p = 5.98\%$, $R_p = 5.78\%$). However, close inspection of the diffraction pattern reveals peak intensities in the calculated pattern for the $Pna2_1$ structure which are not observed in the diffraction data. In addition, the atomic configuration obtained using the $Pna2_1$ model is centrosymmetric, within error (described in detail in the Supporting Information) which is not physically reasonable given the SHG activity of the phase, so the $A2_1am$ structural model is preferred. Full details of the refined structure of $Li_2La(TaTi)O_7$ are given in Table 1, with a plot of the fitted diffraction data shown in Figure 1. Selected bond lengths are given in Table S3 in the Supporting Information. Analysis of analogous NPD data collected from $Li_2La(TaTi)O_7$ at 10 K indicate there are no structural transitions on cooling the sample, as described in the Supporting Information. The polar structure of $Li_2La(TaTi)O_7$ reported here contradicts a previous report of a centrosymmetric structure (space group $Amam$ #63).³⁹ We attribute the difference to the higher spatial resolution of the NPD data collected in the present study.

Structural characterization of $Na_2La(TaTi)O_7$. SXR and NPD data collected from $Na_2La(TaTi)O_7$ were indexed with an orthorhombic unit cell ($a = 5.47$ Å, $b = 5.48$ Å, $c = 20.52$ Å), consistent with an $a' = \sqrt{2}a$, $b' = \sqrt{2}b$, $c' = c$ expansion of an undistorted aristotype, $I4/mmm$ symmetry unit cell of an $n = 2$ Ruddlesden-Popper phase. Refinement of an $A2_1am$ symmetry model, analogous to the refined structure of $Li_2La(TaTi)O_7$, revealed a series of weak diffraction reflections which violate the A-centering extinction conditions. In addition, the refinement indicated that the Na^+ cations are located in the ‘conventional’ 9-coordinate rock salt layer cation sites (in contrast to the Li cations in $Li_2La(TaTi)O_7$). Furthermore, the refined atomic configuration indicated that the $a^-a^-c^0/a^-a^-c^0$ octahedral tilting distortion, described by the X_3^- irreducible representation of the $I4/mmm$ space group, is present in the structure of $Na_2La(TaTi)O_7$, but the $a^0a^0c^+/a^0a^0c^+$ distortion, described by the X_2^+ irreducible representation, is not. Using this information two further models were constructed: an $a^-a^-c^+/a^-a^-(-c^+)$ distortion (X_3^- and X_2^+) in space group $Pnam$ (#62) and an $a^-a^-c^-/a^-a^-(-c^-)$ distortion (X_3^- and X_1^-) in space group $Pnab$ (#60). Refinement of these models against the NPD data revealed that the $Pnab$ model achieved a superior fit to the data and a physically reasonable structure, in contrast to the $Pnam$ model, as described in the Supporting Information. However, measurements revealed that $Na_2La(TaTi)O_7$ is SHG active (activity 0.53 times α - SiO_2) and thus has a non-centrosymmetric crystal structure. This indicated that the structure of $Na_2La(TaTi)O_7$ is subject to a further symmetry-lowering distortion. Thus we considered further distortions of the $Pnab$ model by incorporating polar Γ -point distortion modes generated using the ISODISTORT software.^{33,34} Refinement of these models revealed that the best fit to the data was achieved using a model described in space group $Pna2_1$, which also yielded a physically reasonable structure, as described in the Supporting Information. Displacement parameters of ‘chemically equivalent’ oxide ions (e.g. O(1) + O(2); O(3) + O(4); O(5) + O(6)) were constrained to be the same and those of Ta/Ti(1) and Ta/Ti(2) fixed to prevent negative values. Full details of the refined structure of $Na_2La(TaTi)O_7$ are given in Table 2, with a plot of the fitted diffraction data shown in Figure 2. Selected bond lengths are given in Table S9 in the Supporting Information. Analysis of analogous NPD data collected from $Na_2La(TaTi)O_7$ at 10 K indicate there are no structural transitions on cooling the sample, as described in the Supporting Information.

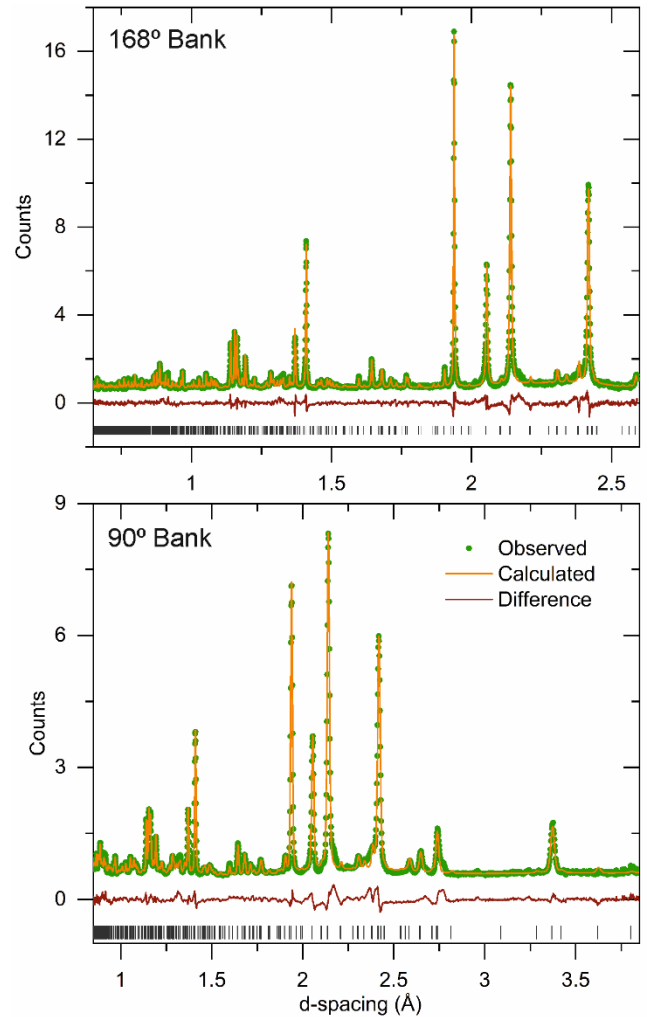


Figure 2. Observed, calculated and difference plots from the structural refinement of $Na_2La(TaTi)O_7$ against NPD data collected at 298 K

Discussion

$Li_2La(TaTi)O_7$ and $Na_2Li(TaTi)O_7$ both adopt $n = 2$ Ruddlesden-Popper structures with polar distortions. However, the mechanism by which the inversion symmetry of the centrosymmetric aristotype $n = 2$ Ruddlesden-Popper structure is broken is qualitatively different for the Li and Na compounds.

$Li_2La(TaTi)O_7$ adopts a structure analogous to the room-temperature phase of $Li_2SrNb_2O_7$,³⁷ in which the lithium cations are located in what is often referred to as the tetrahedral coordination site in the rock salt layers of the framework. However, close inspection reveals that while the lithium cations in $Li_2La(TaTi)O_7$ do have four short bonds (1.99 – 2.16 Å) to the ‘apical’ O(4) oxide ions, there is a further bond of 2.362 Å to an ‘equatorial’ O(3) anion which contributes a bond valence of 0.09 out of a total lithium bond valence sum of 0.92. As a result the lithium cations in $Li_2La(TaTi)O_7$ should be considered to be 5-coordinate, as shown in Figure 3.

The small size of the La^{3+} and Li^+ A-site cations compared to the Ta/Ti B-site cations induces a cooperative tilting distortion to the network of apex-linked (Ta/Ti) O_6 octahedra. As shown

Atom	<i>x</i>	<i>y</i>	<i>z</i>	Occ.	<i>U</i> _{iso}
Na(1)	0.735(3)	0.505(2)	0.8086(4)	1	0.002(1)
Na(2)	0.703(2)	0.507(2)	0.1961(4)	1	0.002(1)
La	0.248(1)	0.998(1)	0.0083(9)	1	0.003(1)
Ta/Ti(1)	0.741(4)	0.478(4)	0.6103(8)	0.5/0.5	0.002*
Ta/Ti(2)	0.731(5)	0.530(4)	0.3961(8)	0.5/0.5	0.002*
O(1)	0.044(2)	0.286(2)	0.4101(10)	1	0.025(1)
O(2)	0.483(3)	0.265(3)	0.6087(10)	1	0.025(1)
O(3)	0.477(2)	0.736(2)	0.4234(9)	1	0.015(1)
O(4)	0.019(2)	0.721(3)	0.5986(6)	1	0.015(1)
O(5)	0.753(2)	0.541(2)	0.3141(9)	1	0.014(2)
O(6)	0.755(2)	0.523(2)	0.7027(9)	1	0.014(2)
O(7)	0.254(3)	0.548(1)	0.0086(10)	1	0.015(2)
Na ₂ La(TaTi)O ₇ – space group <i>Pna</i> 2 ₁ (#33) <i>a</i> = 5.4695(2) Å, <i>b</i> = 5.4813(2) Å, <i>c</i> = 20.5206(8) Å Formula weight = 525.70 g mol ⁻¹ , <i>Z</i> = 4 Radiation source: Neutron Time of Flight Temperature: 298 K <i>w</i> Rp = 7.20%, <i>R</i> p = 6.35%					

Table 2. Parameters from the structural refinement of Na₂La(TaTi)O₇ against NPD data collected at 298 K.

in Figure 3, the (Ta/Ti)O₆ octahedra adopt an out-of-phase $a^-a^-c^0/a^-a^-c^0$ tilting distortion in the *xy*-plane, described by the X_3^- irreducible representation of the *I4/mmm* space group, and an in-phase $a^0a^0c^+/a^0a^0c^+$ distortion around the *z*-axis, described by the X_2^+ irreducible. This combination of tilting distortions ($X_3^- + X_2^+$) yields a structure which cannot be described in a centrosymmetric space group, but which retains inversion symmetry in the arrangement of the atoms. However, the presence of these two distortions modes in combination couple to, and stabilize, the polar Γ_5^- distortion mode via the trilinear coupling mechanism described by Benedek and Fennie,¹⁵ to yield the hybrid-improper polar structure of Li₂La(TaTi)O₇.

The atom displacements arising from the Γ_5^- polar distortion mode, which break the inversion symmetry of the Li₂La(TaTi)O₇ framework, are shown in Figure 3. The displacements occur parallel to the *x*-axis and it can be seen that the direction of the displacements of the Ta/Ti cations is opposite to that of the Li and La cations. Similarly the displacement of the ‘equatorial’ O(2) and O(3) ions oppose the O(1) bridging anion. This shows that Li₂La(TaTi)O₇ should be considered as a ferroelectric, with the overall electrical polarization of the phase arising from a series of opposed, but non-cancelling dipoles, which is a common feature of hybrid-improper ferroelectric phases.

The structure of Na₂La(TaTi)O₇ shares a common La(TaTi)O₇ core with Li₂La(TaTi)O₇, but in contrast to the lithium phase, the Na cations reside in the ‘conventional’ 9-coordinate rock salt layer cation sites. Again the mismatch between the sizes of the La³⁺ and Na⁺ A-site cations and Ta/Ti B-site cations leads to a cooperative tilting of the apex-linked (Ta/Ti)O₆ octahedra. However, in contrast to Li₂La(TaTi)O₇, the *xy*-plane $a^-a^-c^0/a^-a^-c^0$ X_3^- distortion is accompanied by an out of phase $a^0a^0c^-/a^0a^0c^-$ distortion around the *z*-axis in Na₂La(TaTi)O₇ described by the X_1^- irreducible, as shown in Figure 3. This

combination of tilting modes yields a centrosymmetric structure, described in space group *Pnab*, and does not couple to, or stabilize a further polar Γ -point distortion mode via the trilinear coupling mechanism. The stabilization of the Γ_3^- distortion mode, which is observed to lower the structural symmetry of Na₂La(TaTi)O₇ at room temperature, must therefore arise via a different mechanism.

The atom displacements arising from the Γ_3^- polar distortion of Na₂La(TaTi)O₇ are shown in Figure 3. The displacements occur parallel to the *z*-axis and it can be seen that all the cations displace in the same direction (down), while all the anions are displaced in the opposite direction (up). This type of polar displacement is reminiscent of the polar distortions of proper ferroelectric materials, such as BaTiO₃, where the lifting of inversion symmetry is attributed to a SOJT distortion in which the polar displacements of Ti⁴⁺ and O²⁻ ions allows a mixing of the empty Ti 3*d* and filled O 2*p* orbitals, leading to an overall stabilization of the phase.⁴⁻⁷ We propose that an analogous SOJT distortion involving the mixing of the empty Ta 5*d*/Ti 3*d* and filled oxygen 2*p* orbitals drives the Γ_3^- distortion in Na₂La(TaTi)O₇.

The data above show that inclusion of Li or Na leads to a change in the tilting distortion of the La(TaTi)O₇ perovskite double sheets. The tilting distortions of ABO₃ perovskite phases can be generally understood with reference to the Goldschmidt tolerance factor, $t = \langle A-O \rangle / \sqrt{2} \langle B-O \rangle$,⁴⁰ with the degree of distortion generally increasing as *t* declines. However, as noted previously, the situation is more complex in A-cation ordered Ruddlesden-Popper phases such as A¹La(TaTi)O₇ or A¹NdNb₂O₇,^{26,30,41} as the tilting of the octahedral units needs to optimize the local bonding of the two different A-cations simultaneously.

Close inspection shows that the $a^-a^-c^+/a^-a^-c^+$ tilting distortion of Li₂La(TaTi)O₇ efficiently optimizes the coordination sites of the Li⁺ and La³⁺ cations, as indicated by their BVS values (La³⁺ BVS = +3.051; Li⁺ BVS = +0.916).^{42,43} It is clear that replacing Li⁺ with Na⁺ in the *A2₁am* distorted structure would require a significant expansion of the 5-coordinate sites to accommodate the large Na⁺ cations (Li⁺ 4-coordinate radius = 0.59 Å; Na⁺ 4-coordinate radius = 0.99 Å).⁴⁴ This expansion would require a decrease in the magnitude of the tilting distortion, which in turn would expand the 12-coordinate site, occupied by La³⁺, from its optimum size. Thus it is no surprise that Na₂La(TaTi)O₇ adopts a different structure with Na⁺ located in the larger 9-coordinate rock salt sites and an $a^-a^-c^-/a^-a^-c^-$ tilting distortion which allows close to optimum local coordinations for both La³⁺ and Na⁺ (La³⁺ BVS = +2.923; Na⁺ BVS = +0.906/+0.905).

An important consequence of the change in the tilting distortion of the (Ta/Ti)O₆ octahedra on substituting Li⁺ with Na⁺ is that the $a^-a^-c^-/a^-a^-c^-$ distortion, arising from a combination of X_3^- and X_1^- modes, does not stabilize a further Γ -point distortion via the trilinear-coupled hybrid-improper mechanism. This means the observed polar structure of Na₂La(TaTi)O₇ must arise via some other symmetry breaking mechanism, which we attribute to an SOJT distortion driven by the d^0 Ta⁵⁺/Ti⁴⁺ cations. Given that Li₂La(TaTi)O₇ and Na₂La(TaTi)O₇ share a common La(TaTi)O₇ block, the implication is that both A₂La(TaTi)O₇ phases are in principle unstable with respect to a symmetry lowering SOJT distortion, and that the two mechanisms of symmetry breaking (trilinear coupling and SOJT distortion) are in competition, with the Γ -point distortion

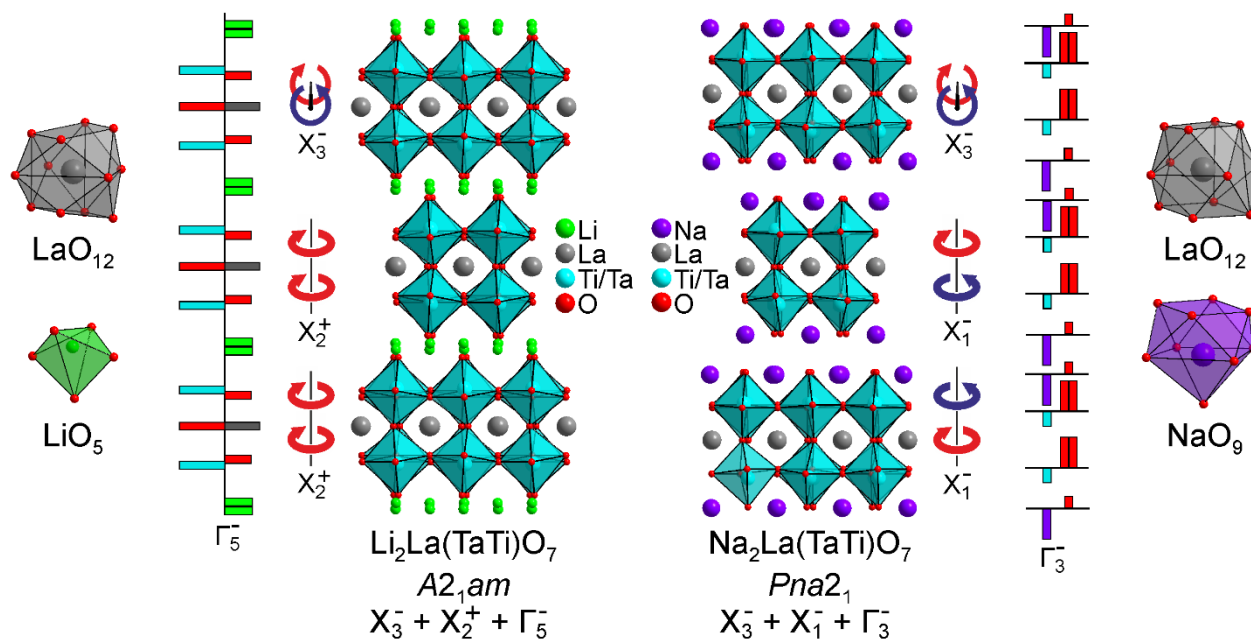


Figure 3. The structures of $\text{Li}_2\text{La}(\text{TaTi})\text{O}_7$ and $\text{Na}_2\text{La}(\text{TaTi})\text{O}_7$ viewed down the $[110]$ direction, the distortion modes which relate these structures to the corresponding undistorted $I4/mmm$ symmetry aristotype structure and the local A-cation coordination polyhedra in the two structures. The lengths of the solid bars represent the magnitudes and relative directions of the displacements of ions due to the Γ -point distortion modes.

which contributes to the ground state structures (trilinear coupling: Γ_5^- ; SOJT: Γ_3^-) controlled by the tilting distortion of the (Ta/Ti) O_6 octahedra, which in turn is directed by the relative size of the A-site cations.

Given that many of the reported hybrid-improper ferroelectric phases derived from layered perovskite oxides contain d^0 transition metals on their B-sites, it is likely that the competition between the hybrid-improper and SOJT symmetry breaking mechanisms observed for $\text{A}_2\text{La}(\text{TaTi})\text{O}_7$ phases is a common feature for many hybrid-improper ferroelectrics. For example, of the $\text{A}'\text{NdNb}_2\text{O}_7$ (A = Li, Na, K, Rb, Cs) series of materials, $\text{LiNdNb}_2\text{O}_7$, $\text{RbNdNb}_2\text{O}_7$ and $\text{CsNdNb}_2\text{O}_7$ adopt polar structures attributable to the trilinear-coupling symmetry-breaking mechanism.^{26, 30, 41} In contrast, the polar structure of KNdNb_2O_7 is attributed to an SOJT distortion of its constituent Nb^{5+}O_6 units. Again this implies the NdNb_2O_7 sheets in all the $\text{A}'\text{NdNb}_2\text{O}_7$ phases are unstable with respect to an SOJT distortion which competes with the trilinear-coupled polar distortions observed for $\text{LiNdNb}_2\text{O}_7$, $\text{RbNdNb}_2\text{O}_7$ and $\text{CsNdNb}_2\text{O}_7$. A similar competition between stabilization mechanisms has recently been reported for $\text{Li}_2\text{SrNb}_2\text{O}_7$.⁴⁵

Conclusion

The lifting of inversion symmetry in the polar structures of $\text{Li}_2\text{La}(\text{TaTi})\text{O}_7$ and $\text{Na}_2\text{La}(\text{TaTi})\text{O}_7$ occurs via two different mechanisms: a trilinear coupled hybrid-improper mechanism for the Li phase and a more conventional SOJT-driven mechanism for the Na phase. The operation of these two different mechanisms in materials with a common $\text{La}(\text{TaTi})\text{O}_7$ core suggests they compete against each other, and further suggests this competition is also occurring in other hybrid-improper ferroelectric phases which contain SOJT active cations, a situation which will clearly have consequences for the preparation of ferroelectric materials of this type.

ASSOCIATED CONTENT

A detailed description of the structural characterization of $\text{Li}_2\text{La}(\text{TaTi})\text{O}_7$ and $\text{Na}_2\text{La}(\text{TaTi})\text{O}_7$ at 298 K and 10 K. A list of selected bond lengths and bond valence sums for $\text{Li}_2\text{La}(\text{TaTi})\text{O}_7$ and $\text{Na}_2\text{La}(\text{TaTi})\text{O}_7$. This material is available free of charge via the Internet at <http://pubs.acs.org>.

AUTHOR INFORMATION

Corresponding Author

michael.hayward@chem.ox.ac.uk

Author Contributions

The manuscript was written through contributions of all authors.

ACKNOWLEDGMENT

Experiments at the Diamond Light Source were performed as part of the Block Allocation Group award "Oxford/Warwick Solid State Chemistry BAG to probe composition-structure-property relationships in solids" (EE18786). Experiments at the ISIS pulsed neutron facility were supported by a beam time allocation from the STFC (RB 2000148). SM thanks Somerville College for an Oxford Ryniker Lloyd scholarship. PSH and WZ thank the Welch Foundation (Grant E-1457) for support.

REFERENCES

- Lines, M. E.; Glass, A. M., *Principles and Applications of Ferroelectrics and Related Materials*. Oxford University Press: Oxford, 1991.
- Nye, F. J., *Physical Properties of Crystals*. Oxford University Press: Oxford, UK, 1957.
- Halasyamani, P.; Poeppelmeier, K. R., Noncentrosymmetric oxides. *Chem. Mater.* **1998**, *10*, 2753-2769.
- Cohen, R. E., Origin of Ferroelectricity in Perovskite Oxides. *Nature* **1992**, *358* (6382), 136-138.
- Kang, S. K.; Tang, H.; Albright, T. A., Structures for d^0 Ml_6 and Ml_5 Complexes. *J. Am. Chem. Soc.* **1993**, *115* (5), 1971-1981.
- Kunz, M.; Brown, I. D., Out-of-Center Distortions around Octahedrally Coordinated d^0 Transition-Metals. *J. Solid State Chem.* **1995**, *115* (2), 395-406.

7. Pearson, R. G., The 2nd-Order Jahn-Teller Effect. *Theochem-Journal of Molecular Structure* **1983**, 12 (AUG), 25-34.
8. Lefebvre, I.; Lannoo, M.; Allan, G.; Ibanez, A.; Fourcade, J.; Jumas, J. C.; Beaurepaire, E., Electronic-Properties of Antimony Chalcogenides. *Phys. Rev. Lett.* **1987**, 59 (21), 2471-2474.
9. Lefebvre, I.; Szymanski, M. A.; Olivier-Fourcade, J.; Jumas, J. C., Electronic Structure of Tin Monochalcogenides from SnO to SnTe. *Phys. Rev. B* **1998**, 58 (4), 1896-1906.
10. Seshadri, R.; Hill, N. A., Visualizing the Role of Bi 6s "Lone Pairs" in the Off-Center Distortion in Ferromagnetic BiMnO₃. *Chem. Mater.* **2001**, 13 (9), 2892-2899.
11. Stoltzfus, M. W.; Woodward, P. M.; Seshadri, R.; Klepeis, J. H.; Bursten, B., Structure and Bonding in SnWO₄, PbWO₄, and BiVO₄: Lone Pairs vs Inert Pairs. *Inorg. Chem.* **2007**, 46 (10), 3839-3850.
12. Watson, G. W.; Parker, S. C., Origin of the Lone Pair of alpha-PbO from Density Functional Theory Calculations. *J. Phys. Chem. B* **1999**, 103 (8), 1258-1262.
13. Watson, G. W.; Parker, S. C.; Kresse, G., Ab Initio Calculation of the Origin of the Distortion of Alpha-PbO. *Phys. Rev. B* **1999**, 59 (13), 8481-8486.
14. Hill, N. A., Why Are There So Few Magnetic Ferroelectrics? *J. Phys. Chem. B* **2000**, 104, 6694-6709.
15. Benedek, N. A.; Fennie, C. J., Hybrid Improper Ferroelectricity: A Mechanism for Controllable Polarization-Magnetization Coupling. *Phys. Rev. Lett.* **2011**, 106 (10), 107204.
16. Mulder, A. T.; Benedek, N. A.; Rondinelli, J. M.; Fennie, C. J., Turning ABO₃ Antiferroelectrics into Ferroelectrics: Design Rules for Practical Rotation-Driven Ferroelectricity in Double Perovskites and A₃B₂O₇ Ruddlesden-Popper Compounds. *Advanced Functional Materials* **2013**, 23 (38), 4810-4820.
17. Benedek, N. A.; Mulder, A. T.; Fennie, C. J., Polar octahedral rotations: A path to new multifunctional materials. *J. Solid State Chem.* **2012**, 195, 11-20.
18. Rondinelli, J. M.; Fennie, C. J., Octahedral Rotation-Induced Ferroelectricity in Cation Ordered Perovskites. *Adv. Mater.* **2012**, 24 (15), 1961-1968.
19. King, G.; Woodward, P. M., Cation Ordering in Perovskites. *J. Mater. Chem.* **2010**, 20, 5785-5796.
20. Anderson, M. T.; Greenwood, K. B.; Taylor, G. A.; Poeppelmeier, K. R., B-cation arrangements in double perovskites. *Prog. Solid St. Chem.* **1993**, 22, 197-233.
21. Oh, Y. S.; Luo, X.; Huang, F. T.; Wang, Y. Z.; Cheong, S. W., Experimental demonstration of hybrid improper ferroelectricity and the presence of abundant charged walls in (Ca, Sr)₃Ti₂O₇ crystals. *Nat. Mater.* **2015**, 14 (4), 407-413.
22. Yoshida, S.; Akamatsu, H.; Tsuji, R.; Hernandez, O.; Padmanabhan, H.; Sen Gupta, A.; Gibbs, A. S.; Mibu, K.; Murai, S.; Rondinelli, J. M.; Gopalan, V.; Tanaka, K.; Fujita, K., Hybrid Improper Ferroelectricity in (Sr,Ca)₃Sn₂O₇ and Beyond: Universal Relationship between Ferroelectric Transition Temperature and Tolerance Factor in *n* = 2 Ruddlesden-Popper Phases. *J. Am. Chem. Soc.* **2018**, 140 (46), 15690-15700.
23. Yoshida, S.; Fujita, K.; Akamatsu, H.; Hernandez, O.; Sen Gupta, A.; Brown, F. G.; Padmanabhan, H.; Gibbs, A. S.; Kuge, T.; Tsuji, R.; Murai, S.; Rondinelli, J. M.; Gopalan, V.; Tanaka, K., Ferroelectric Sr₃Zr₂O₇: Competition between Hybrid Improper Ferroelectric and Antiferroelectric Mechanisms. *Advanced Functional Materials* **2018**, 28 (30), 1801856.
24. Liu, M. F.; Zhang, Y.; Lin, L. F.; Lin, L.; Yang, S. W.; Li, X.; Wang, Y.; Li, S. Z.; Yan, Z. B.; Wang, X. Z.; Li, X. G.; Dong, S.; Liu, J. M., Direct observation of ferroelectricity in Ca₃Mn₂O₇ and its prominent light absorption. *Appl. Phys. Lett.* **2018**, 113 (2), 022902.
25. Benedek, N. A., Origin of Ferroelectricity in a Family of Polar Oxides: The Dion-Jacobson Phases. *Inorg. Chem.* **2014**, 53 (7), 3769-3777.
26. Zhu, T.; Cohen, T.; Gibbs, A. S.; Zhang, W.; Halasyamani, P. S.; Hayward, M. A.; Benedek, N. A., Theory and Neutrons Combine To Reveal a Family of Layered Perovskites without Inversion Symmetry. *Chem. Mater.* **2017**, 29 (21), 9489-9497.
27. Zhu, T.; Gibbs, A. S.; Benedek, N. A.; Hayward, M. A., Complex Structural Phase Transitions of the Hybrid Improper Polar Dion-Jacobson Oxides RbNdM₂O₇ and CsNdM₂O₇ (M = Nb, Ta). *Chem. Mater.* **2020**, 32 (10), 4340-4346.
28. Asaki, S.; Akamatsu, H.; Hasegawa, G.; Abe, T.; Nakahira, Y.; Yoshida, S.; Moriyoshi, C.; Hayashi, K., Ferroelectricity of Dion-Jacobson layered perovskites CsNdNb₂O₇ and RbNdNb₂O₇. *Jpn. J. Appl. Phys.* **2020**, 59 (SP), 6.
29. Benedek, N. A.; Rondinelli, J. M.; Djani, H.; Ghosez, P.; Lightfoot, P., Understanding Ferroelectricity in Layered Perovskites: New Ideas and Insights From Theory and Experiments. *Dalton Trans.* **2015**, 44 (23), 10543-10558.
30. Zhu, T.; Khalsa, G.; Havas, D. M.; Gibbs, A. S.; Zhang, W.; Halasyamani, P.; Benedek, N. A.; Hayward, M. A., Cation Exchange as a Mechanism to Engineer Polarity in Layered Perovskites. *Chem. Mater.* **2018**, 30, 8915-8924.
31. Coelho, A. A. *TOPAS Academic: General profile and Structure Analysis Software For Powder Diffraction Data*, Bruker AXS, Karlsruhe, Germany: 2016.
32. Ok, K. M.; Chi, E. O.; Halasyamani, P. S., Bulk characterization methods for non-centrosymmetric materials: second-harmonic generation, piezoelectricity, pyroelectricity, and ferroelectricity. *Chem. Soc. Rev.* **2006**, 35, 710-717.
33. Campbell, B. J.; Stokes, H. T.; Tanner, D. E.; Hatch, D. M., ISODISPLACE: a web-based tool for exploring structural distortions. *J. Appl. Crystallogr.* **2006**, 39, 607-614.
34. Stokes, H. T.; Hatch, D. M.; Campbell, B. J. *ISOTROPY Software Suite*, iso.byu.edu, 2007.
35. Glazer, A. M., Classification of tilted Octahedra in Perovskites. *Acta Crystallogr. Sect. B-Struct. Commun.* **1972**, B 28 (NOV15), 3384-3392.
36. Woodward, P. M., Octahedral tilting in perovskites .1. Geometrical considerations. *Acta Crystallogr. Sect. B-Struct. Commun.* **1997**, 53, 32-43.
37. Uppuluri, R.; Akamatsu, H.; Sen Gupta, A.; Wang, H. Y.; Brown, C. M.; Lopez, K. E. A.; Alem, N.; Gopalan, V.; Mallouk, T. E., Competing Polar and Antipolar Structures in the Ruddlesden-Popper Layered Perovskite Li₂SrNb₂O₇. *Chem. Mater.* **2019**, 31 (12), 4418-4425.
38. Nagai, T.; Shirakuni, H.; Nakano, A.; Sawa, H.; Moriwake, H.; Terasaki, I.; Taniguchi, H., Weak Ferroelectricity in *n*=2 Pseudo Ruddlesden-Popper-Type Niobate Li₂SrNb₂O₇. *Chem. Mater.* **2019**, 31 (16), 6257-6261.
39. Fanah, S. J.; Yu, M.; Huq, A.; Ramezanipour, F., Insight into lithium-ion mobility in Li₂La(TaTi)O-7. *Journal of Materials Chemistry A* **2018**, 6 (44), 22152-22160.
40. Goldschmidt, V. M., Die Gesetze der Krystallochemie. *Naturwissenschaften* **1926**, 14, 477-485.
41. Mallick, S.; Gibbs, A. S.; Zhang, W. G.; Halasyamani, P. S.; Benedek, N. A.; Hayward, M. A., Polar Structures of KNdNb₂O₇ and KNdT₂O₇. *Chem. Mater.* **2020**, 32 (18), 7965-7972.
42. Brese, N. E.; O'Keeffe, M., Bond-Valence Parameters for Solids. *Acta Crystallogr., Sect. B : Struct. Sci.* **1991**, B47, 192-197.
43. Brown, I. D.; Altermatt, D., Bond-Valence Parameters Obtained from a Systematic Analysis of the Inorganic Crystal Structure Database. *Acta Crystallogr., Sect. B : Struct. Sci.* **1985**, B41, 244-247.
44. Shannon, R. D., Revised effective ionic radii. *Acta Cryst.* **1976**, A32, 751-766.
45. Mochizuki, Y.; Nagai, T.; Shirakuni, H.; Nakano, A.; Oba, F.; Terasaki, I.; Taniguchi, H., Coexisting Mechanisms for the Ferroelectric Phase Transition in Li₂SrNb₂O₇. *Chem. Mater.* **2021**, 33, 1257-1264.

